Thermal Properties of the LHCb VELO Silicon Sensors

Internal Note

Issue:	1
Revision:	0
Reference:	LHCb-2007-099
Created:	March 6, 2007
Last modified:	June 25, 2007

Prepared by: Thijs Versloot[a], Ann Van Lysebetten[a]
[a]NIKHEF,The Netherlands

Abstract

This note reports on the thermal measurements performed on the first VELO production modules and on a test module with TPG inserts for improvement of the thermal coupling. The thermal behaviour of the modules and their cooling performance was tested in both dry air and under vacuum operation. The measurements showed that the CO_2 cooling system is able to provide the required operating conditions of the module (<0 °C). Thermal images of the VELO silicon showed a direct relation between the silicon temperature and the temperature sensors on the hybrid. A slight thermal improvement (1.6 °C) was found when comparing vacuum operation of the test module with and without inserts.

Document Status Sheet

1. Document Title: Thermal Properties of the LHCb VELO Silicon Sensors			
2. Document Reference Number: LHCb-2007-099			
3. Issue	**4. Revision**	**5. Date**	**6. Reason for change**
Draft	1	September 8, 2006	First version. Summer Student Project report
Draft	2	March 6, 2007	Conversion to LHCb Internal Note
Draft	3	June 20, 2007	Grammar check and submission

Contents

1 Introduction

The VELO [1] features a total of 42 double-sided silicon modules and 4 pile-up silicon modules, installed in two halves. During detector operation, heat is produced in the electronic elements on the module hybrids. The silicon temperature should stay at all times below 0 °C to delimit the effects of radiation damage. The position of the VELO, close to the LHC beam and in vacuum (10^{-4} mbar), requires direct thermal cooling with a radiation resistant refrigerant. The cooling system must be able to handle a total heat load of up to 2.5 kW. The chosen refrigerant for the VELO cooling system is two-phase CO_2, which is cooled by a conventional freon cooler. The CO_2 is transported by a 60 m long transfer line from the cooling platform to the VELO, where it is distributed over 27 capillaries per detector half. Each capillary will cool a module through 5 cooling blocks attached to the module. The cooling system is described in more detail in [2, 3]. Figure 1 gives a horizontal cross section view of the modules of one detector half.

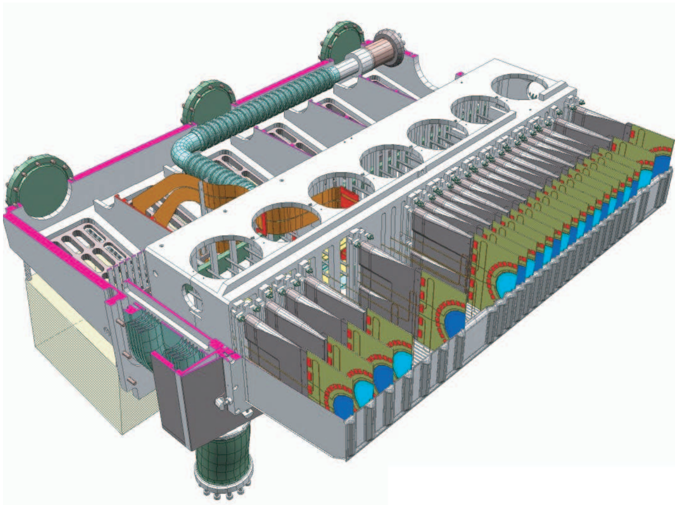

Figure 1 Detailed drawing of right detector half with mounted silicon sensors and partly visible RF-foil and cooling system.

In this note, the results of a study on the cooling performance are presented. A relationship between the temperature measured with a thermal camera and the temperature measured on the hybrid board is established (see Section 3.1). The cooling performance was tested for one module (see Section 3.2) and potential cooling improvements have been investigated (see Section 3.3).

2 Experimental Setup

The layout of a VELO module is depicted in Fig. 2(a). The silicon(1) is attached to an electric circuit board(2, the hybrid) to form a sensor. Two sensors are mounted back to back on a central support(3). This central support is made from Thermo-Pyrolythic-Graphite (TPG) that conducts heat effectively (1700 $\mathrm{Wm^{-1}K^{-1}}$) throughout the hybrid. The two sensors and central support are then mounted on the paddle(5) that is finally attached to the base of detector half with a foot(6). The main heat production on the module is located at the Beetle chips around the silicon sensors, generating a total heat load of approximately 0.75 W per chip ($\sim$ 24 W for a fully powered module). Two temperature sensors (Negative Temperature Coefficients, NTC) are installed on the hybrid (shown in Fig. 3) to monitor the local temperature. These temperatures are read out by the Temperature board and can be monitored.

During assembly and commissioning of the VELO modules on the detector base in the lab a CO_2 cooling system [4] was used. This system can cool up to five modules with a total maximum mass flow of 3 g/s and works according to the same principle as the final cooling apparatus, which is under construction at NIKHEF. The CO_2 from a bottle (at a pressure of $\sim$60 bar) goes through calibrated restrictions which regulate the flow. The setpoint temperature or temperature at which the modules will be cooled

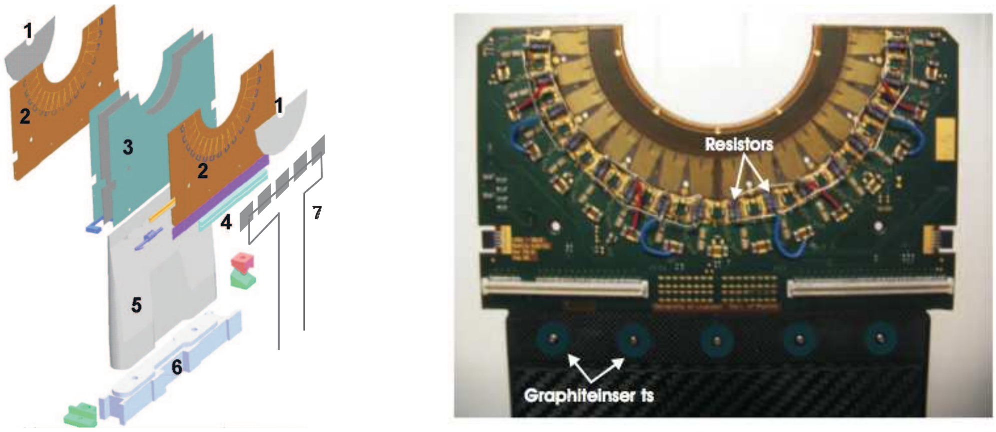

(a) (b)

Figure 2 (left) Schematic drawing and components of a VELO module. (right) Electrical module used in the measurements. The Beetle chips are replaced by resistors and on one side of the module, the TPG inserts are visible at the cooling connection.

is set by the expansion pressure in the system, it can vary from ∼12.5 to 37 bar which corresponds to setpoint temperatures from -40 to 0 °C. The CO_2 is then expanded over the capillaries going to each individual module. These capillaries with an inner diameter of 0.9 mm [5] run through cooling pads (each module has 5 *"cookies"*, see(7) in Fig. 2(a)) directly attached to the hybrid by captive screws and a layer of Thermflow [6]. Thermflow is a phase-change thermal interface material with a low thermal impedance (0.7 $Wm^{-1}K^{-1}$) maximising the heat sink performance. This performance is only obtained after having applied a specific melting procedure. In these test the Thermflow was unmelted, reducing the performance by a few degrees. The exhaust CO_2 is heated above room temperature and vented outside. Throughout the blow system and on the evaporator, PT100 sensors are installed to monitor the temperatures during operation.These are read out by the HAPTAS and a Labview program.
In this study, the temperature of one module side was also measured with a thermal camera (FLIR ThermaCam E45). The calibration measurements were performed on black body radiation at known temperatures to extract the setup coefficients (e.g. the emissivities and transmission constants of the various module components). Furthermore, the additional optical components in the setup (e.g the quartz window) need to be taken into account. Therefore, a Matlab analysis program, 'SathPict' [7], was specially written to perform this full calibration and obtain the absolute temperature of the components (see Fig. 3). The uncertainty on the camera measurement is ±1.5 °C. The local temperatures measured with the thermoresistors have an uncertainty of ±0.1 °C.

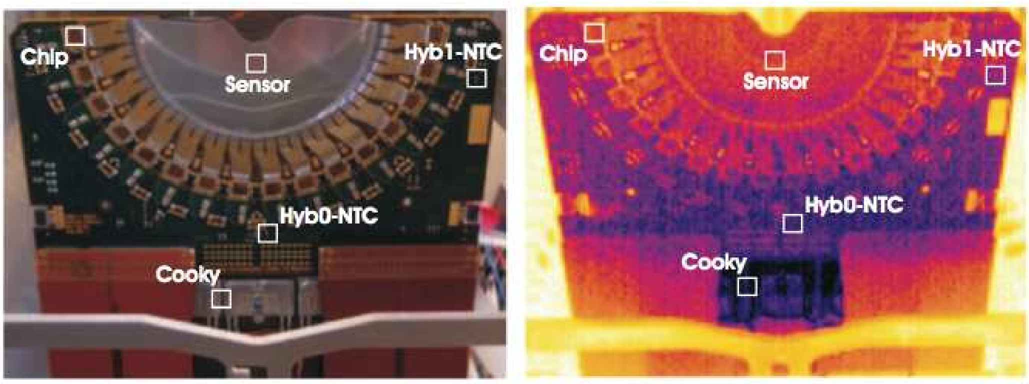

Figure 3 Normal(left) and Thermal(right) image of a mounted module. In the images, the analysed areas are shown for which the average temperature is calculated. The location of the NTCs (NTC_0 at the top and NTC_1 at the base near the cooling pad) on the hybrid have also been marked in both images.

For the tests described in this note two types of modules were used. The first was a fully mounted pre-production module (M14) complete with silicon and readout chips. The second one was an electrical test module (see Fig. 2(b)). This test module does not contain silicon sensors and the Beetle chips are replaced by soldered resistors with a total resistance of R = 10.8 Ω. Under normal operation, a comparable heat load can thus be produced to test the cooling performance (measured at $\sim$ 17 W when both sides are powered). The test module is also fitted with graphite (TPG) inserts as indicated on Fig. 2(b). Five graphite disks of 10 mm diameter and 250 μm thick are inserted on one side of the hybrid at the positions of the cooling cookie connection. These inserts should further improve the direct thermal coupling to the hybrid. We will compare our results obtained with the thermal studies to measurements carried out by Liverpool [8].

The measurements described here were performed in both dry-air and vacuum close to the final experimental conditions (10^{-3} mbar). The modules were fully powered on both sides. No thermal camera images can be made during vacuum test for technical reasons. Furthermore, the temperatures were recorded when the cooling setup has reached a stable equilibrium. Both the NTC temperatures and the camera measurements were taken at the same time. Fig. 4 shows the thermal camera images of the pre-production module when cooled down to -25 °C with the Beetle chips unpowered (left) and the image of a fully powered and cooled module (right).

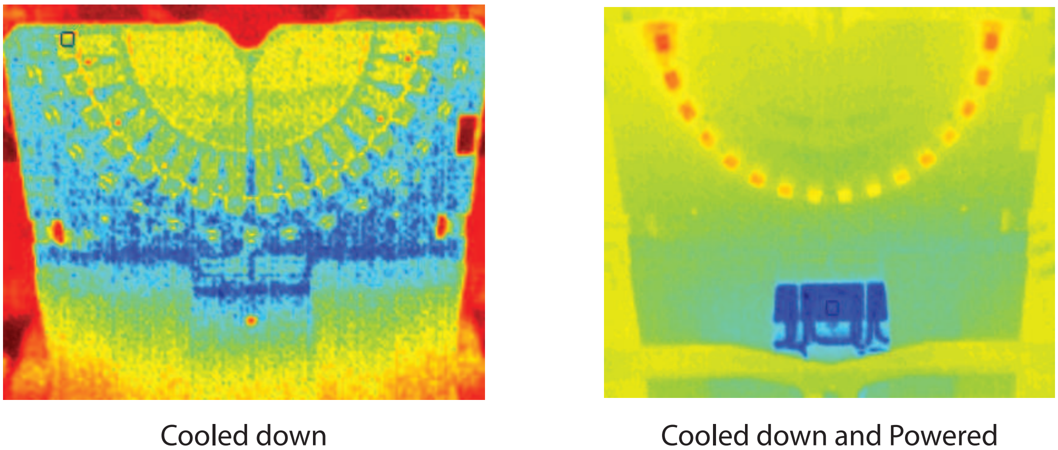

Figure 4 Thermal camera images of the pre-production module during dry-air operation. The left image shows the module cooled down at a cooling temperature of -25 °C, consecutively the module is fully powered in the right image. Notice the clearly visible Beetle chips and cooling pad when the module is fully powered and after the cooling system has stabilised.

3 Measurements & Analysis

3.1 Relation between the temperatures measured by the NTCs and the silicon

No thermoresistors can be placed on the silicon surface to measure the temperature. The closest available temperature measurement is by the NTC on the hybrid board close to the top Beetle chip (NTC_1). In this section the relation between top NTC and silicon temperature will be investigated. This can only be obtained when the thermal camera provides an accurate temperature measurement. The temperature measured by the top NTC (NTC_1, represented by squares) as function of the cooling set point temperature is shown in Fig. 5(a). A linear relation is fitted to these data points indicated in the figure. This figure also contains the temperatures measured with the thermal camera on the top NTC location (represented by circles), defined as hyb1 in Figure 3, during dry air operation with both sides of the module powered. For the range of cooling temperatures shown here it is seen that the thermal camera measurement agrees well with the temperature measured by the NTC. It can be concluded that the thermal camera is well calibrated and gives an accurate absolute temperature.
Figure 5(b) shows the camera measurements for the two NTCs versus the temperature of the silicon surface measured by the thermal camera during dry air operation. To obtain different silicon temperatures, the cooling set point temperature was varied between -10 °C and -40 °C. The data points for the top NTC(NTC_1) are fitted with a linear relationship. Combining the thermal results with the NTC readout, the NTC_1 measurement was seen to be a good indicator of the silicon temperature during dry air operation.

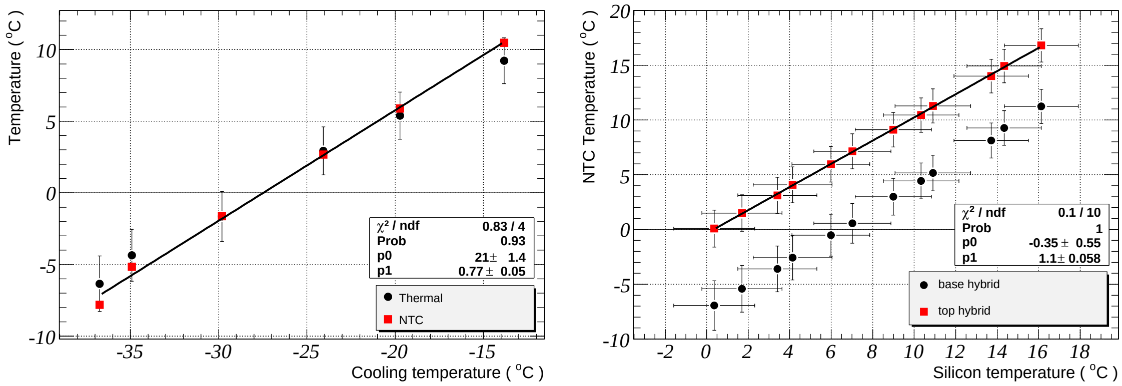

(a) (b)

Figure 5 a) Cooling results for operation without TPG inserts in dry air, measured with camera and NTC. Results are from the top NTC with all resistors on both sides of the module powered. b) Relationship between NTC temperature (NTC_0 or base hybrid represented by circles and NTC_1 top hybrid represented by squares) and silicon temperatures measured by the thermal camera.

3.2 Cooling performance

In this section the cooling performance on a pre-production module is verified for a standard setpoint temperature of -25 °C and a temperature range around this setpoint temperature. Fig. 4 shows a thermal image of the pre-production module cooled at -25 °C and powered. In this case the Beetle chips are clearly visible. Figure 6(a) displays the temperature measured by the thermal camera at the various module components (as defined in Fig. 3) as a function of the cooling set point temperature varying between -37 °C and -14 °C. Both sides of the module were powered and the test was carried out in dry air on the production module. It can be seen that for a cooling setpoint below -30 °C, the top NTC temperature was measured to drop below 0 °C. The temperature of the top most readout chip was used as the Beetle temperature. Furthest away from the cooling connection, this chip will reach the highest temperature. Unpowered, the temperatures of the Beetle chip, NTC_1 and NTC_0 reach respectively -9, -11 and -15 °C at a -25 °C cooling setpoint temperature. When the chips are powered, the temperature difference between the two NTCs increases by a factor two and the temperature drop

between cooling cookie and NTC_0 is approximately 27 °C as is shown in Fig. 6(a).
The silicon temperature measured by NTC_1 against the cooling setpoint temperature is shown in Fig. 6(b). This figure contains the measurements in both dry-air (represented by triangles) and vacuum conditions (represented by squares). The vacuum data points are fitted with a straight line, the results are displayed in the figure. These results show a marginally larger gradient than the dry air results. At a cooling set point temperature of -30 °C the top NTC temperature was measured to be approximately -2 °C during both dry air and vacuum operation.

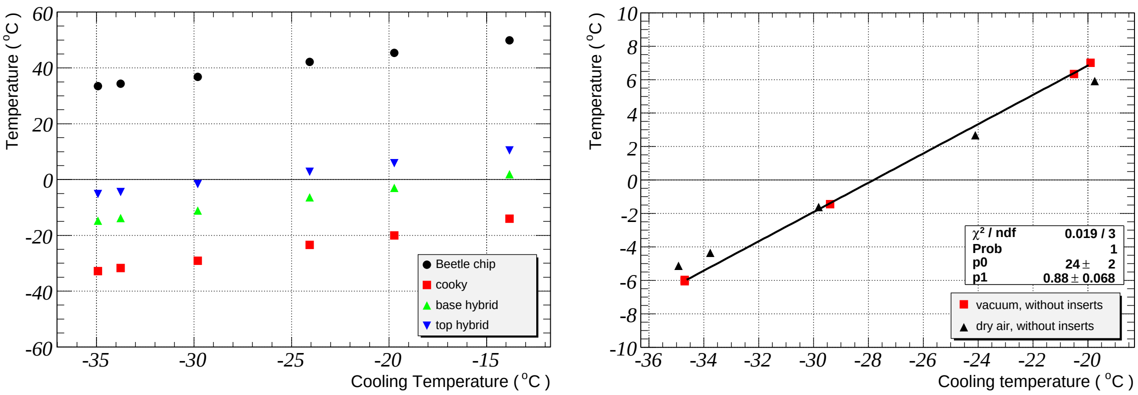

(a) (b)

Figure 6 (a) The temperature measurements of hybrid components (measured with the thermal camera) versus the cooling setpoint temperature. (b) NTC measurements for operation without TPG inserts in dry air and vacuum (10^{-3} mbar) conditions.

3.3 Cooling performance with TPG inserts

To verify eventual improvements in the cooling performance the dry air and vacuum measurements were repeated on the electronic module with TPG inserts at the cooling connections (see Fig. 7(b)). The NTC_1 measurement against cooling setpoint temperature for both dry air (represented by triangles) and vacuum operation (represented by circles) are shown in Fig. 7(a). A straight line is fitted through the data points obtained in vacuum. The addition of inserts lowered the temperature at the top NTC by approximately 1 °C in dry air, while in a vacuum (10^{-3} mbar) a marginal improvement of $\sim$ 2 °C is observed. At a cooling set point temperature of -30 °C, the top NTC temperature was measured to be -2.7 °C in dry air and -4.3 °C under vacuum conditions.

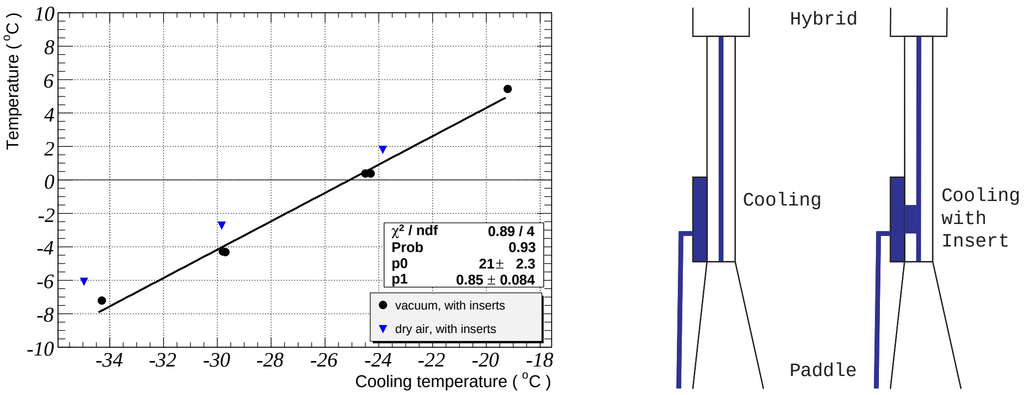

(a) (b)

Figure 7 a) NTC measurements for operation with TPG inserts in dry air and vacuum (10^{-3} mbar) condition. b) Schematic cross section with and without TPG inserts at the module base.

4 Conclusions

The thermal properties of a pre-production module were measured and results show that the design operating temperature can be well reached with a cooling temperature of -30 °C under vacuum operation. During these tests the Thermflow was not melted according to the specifications, hence an additional improvement of a few degrees is expected with melted Thermflow and these results can probably be reach at a somewhat higher cooling setpoint temperature. In a further study the influence of the neighbouring modules should also be taken into account.
The thermal camera showed that the silicon surface temperature is approximately homogeneous in dry air operation. The comparison of the silicon temperature with the thermal camera to the NTC_1 measurement, also showed a linear relationship well within the error bars.
The temperature difference between the cooling set point and the top NTC increased from 25 to 30 °C when varying the cooling setpoint temperature from -20 to -35 °C. Furthermore, the temperature difference between the base and top NTC increases from 8 to 11 °C. The largest temperature drop is located at the cooling connection at the base of the hybrid. This could be overcome by a better connection.
An electrical test module with TPG inserts was used to investigate the possible improvement in the direct thermal contact. The measurements showed a marginal improvement of ~ 1 °C in dry air and ~ 2 °C under vacuum (10^{-3} mbar) conditions. In the real experiment, the vacuum will be a factor 10-100 lower which would further reduce the radiation losses. The above mentioned cooling improvements are consistent with the measurements performed in Liverpool [8]. A possible explanation for the marginal improvement could be the relatively small area of the inserts compared to the total cooling pad size (392 mm^2 compared to the total area of 1520 mm^2). Increasing the contact area could therefore improve the cooling performance of the modules.

Acknowledgments

We are indebted to Raphael Dumps, without his technical assistance these measurements would not have been possible. We would also like to thank Stefan Rosseger for his contribution to the calibration of the thermal camera and for providing the thermal analysis program.

5 References

[1] LHCb collaboration, *LHCb VELO Technical Design Report*, CERN/LHCC 2001-0011, 5, 2001

[2] B. Verlaat, *Controlling a secondary 2-phase* CO_2 *loop using a 2-phase accumulator*, International Congress of Refrigeration, ICR07-B2-1565, Beijing, 2007

[3] B. Verlaat, *Thermal Performance Testing of the VTCS Evaporator and VELO Module*, NIKHEF, EN 05-01, 2005

[4] *How to operate blowsystem*,
available at: https://uimon.cern.ch/twiki/bin/view/LHCb/VeloBlowSystem, 2006-06-19

[5] LHCb collaboration, *LHCb Re-optimized Detector Design and Performance*, CERN/LHCC 2003-030, 9, 2003

[6] http://www.chomerics.com/products/documents/TB77page.pdf

[7] S. Rosseger, *Thermal Studies of the LHCb Vertex Locator using Non-Destructive IR Thermography*, Diploma Thesis, Graz Uni. of Tech., 2006.

[8] G. Casse, R. Oldeman, T. Smith, *Thermal test of LHCb VELO module 14 and test of TPG inserts*, Liverpool documentation, 22 May 2006.